Isomeric separation of cannabinoids by UPLC combined with ionic mobility mass spectrometry (TWIM-MS)-Part I

Tose, Lilian V.; Santos, Nayara A.; Rodrigues, Rayza R T; Murgu, Michael; Gomes, Alexandre F.; Vasconcelos, Géssica A.; Souza, Paulo C T; Vaz, Boniek G.; Romão, Wanderson

Published in:
International Journal of Mass Spectrometry

DOI:
10.1016/j.ijms.2016.10.018

Document Version
Publisher's PDF, also known as Version of record

Publication date:
2017

International Journal of Mass Spectrometry 418 (2017) 112–121

Contents lists available at ScienceDirect

International Journal of Mass Spectrometry

journal homepage: www.elsevier.com/locate/ijms

Isomeric separation of cannabinoids by UPLC combined with ionic mobility mass spectrometry (TWIM-MS)—Part I

Lilian V. Tose[a], Nayara A. Santos[a], Rayza R.T. Rodrigues[a], Michael Murgu[b], Alexandre F. Gomes[b], Géssica A. Vasconcelos[c], Paulo C.T. Souza[d], Boniek G. Vaz[c], Wanderson Romão[a,e,*]

[a] Petroleomic and Forensic Chemistry Laboratory, Department of Chemistry, Federal University of Espírito Santo, 29075-910 Vitória, ES, Brazil
[b] WatersTechnologies of Brazil, Alameda Tocantins 125, 27° Andar, Barueri, SP CEP 06455-020, Brazil
[c] Chemistry Institute, Federal University of Goiás, 74001-970 Goiânia, GO, Brazil
[d] Faculty of Mathematics and Natural Sciences, University of Groningen, Groningen, Netherlands
[e] Federal Institute of Education, Science and Technology of Espírito Santo, 29106-010 Vila Velha, ES, Brazil

ARTICLE INFO

Article history:
Received 28 June 2016
Received in revised form 12 October 2016
Accepted 27 October 2016
Available online 29 October 2016

Keywords:
Cannabinoids
Isomers
Δ^9-THC
Uplc-twim-ms
Ionic mobility

ABSTRACT

The *Cannabis sativa* L. plant is rich in a wide variety of cannabinoids. Δ^9–tetrahydrocannabinol (Δ^9–THC) is the main chemical compound responsible for its psychoactive effect, and it can be identified as $[M+H]^+$ and $[M-H]^-$ ions at *m/z* 315 and 313, respectively, where $M = C_{21}H_{30}O_2$. However, six other isomeric or isobaric forms of Δ^9–THC can exist, which makes its unequivocal characterization a challenge. In this work, ultra-high liquid chromatography coupled to traveling wave ion mobility mass spectrometry (UPLC-TWIM-MS) were applied to both electrospray ionization modes (ESI(±)) and used to analyze hashish, marijuana, and parts of the *Cannabis Sativa* L. plant (flower and leaf). The presence of a complex isomeric mixture of cannabinoids has been identified, and the mixture mainly contains Δ^9-THC, cannabidiol (CBN-C_5 and M_w = 310 Da), Δ^9-tetrahydrocannabinolic acid A and B (Δ^9-THCA-C_5 A/B and M_w = 358 Da) and their isomers. Three isomers of the ions were identified at *m/z* 315/313, 311, and 357 by using direct infusion ESI-TWIM-MS technique, while higher selectivity was observed in UPLC-ESI-TWIM-MS data, with the maximum isomeric separation between four and five compounds achieved when using single-ion mode (SIM) acquisition. The ions at *m/z* 311/309, 315/313, 345, and 357 correspond to CBN-C_5, Δ^9-THC, cannabielsioc acid, Δ^9-THCA-C_5 and their isomers, respectively, and they were the main species found. The calculations of collision cross sections were reported for all isomers of cannabinoids and associated with TWIM-MS results.

1. Introduction

Marijuana is originates from the *Cannabis sativa* L. plant [1,2], which contains many different natural compounds, of which more than 535 have already been identified and 70 are cannabinoids. These cannabinoids are responsible for the plant's physiological and psychological effects, and they are classified into two groups: psychoactive (Δ^8-tetrahydrocannabinol, and Δ^9-tetrahydrocannabinol(Δ^9-THC)) and non-psychoactive (cannabinol, CBN, canabidiol (CBD), etc.) [3,4]. The term cannabinoid is attributed to the group of molecules composed of 21 carbon atoms present in the *Cannabis sativa* L. plant and the products of their transformation [1,5,6].

In addition to Δ^9-THC (M_w = 314 Da), five other isomers of Δ^9-THC can exist in marijuana samples: Δ^9-6aS,10aR-*cis*-tetrahydrocannabinol ((−)-*cis*- Δ^9-THC), Δ^8-*trans*-(6aR,10aR)-tetrahydrocannabinol (Δ^8-*trans*-THC), (±)-1aS,3aR,8bR,8cR-cannabicyclol (CBL-C_5), cannabichromene (CBC-C_5), and cannabidiol (CBD-C_5) (see in Fig. 1a). Among them, CBD-C_5 constitutes up to 40% of cannabis extracts and is responsible for the typical psychological effects of cannabis in humans. In general, it has anxiolytic and/or antipsychotic actions [7], whereas most of the other isomers of Δ^9-THC exhibit non-biological activity [8].

The main natural precursor of Δ^9-*trans*-THC-C_5 is Δ^9-THCA-C_5 A/B (Δ^9-tetrahyrocannabinolic acid A and B, M_w = 358 Da), Fig. 1b, and it does not have psychotropic effects. Δ^9-THCA can undergo

* Corresponding author at: Federal Institute of Education, Science and Technology of Espírito Santo, 29106-010 Vila Velha, ES, Brazil.
E-mail address: wandersonromao@gmail.com (W. Romão).

http://dx.doi.org/10.1016/j.ijms.2016.10.018
1387-3806/

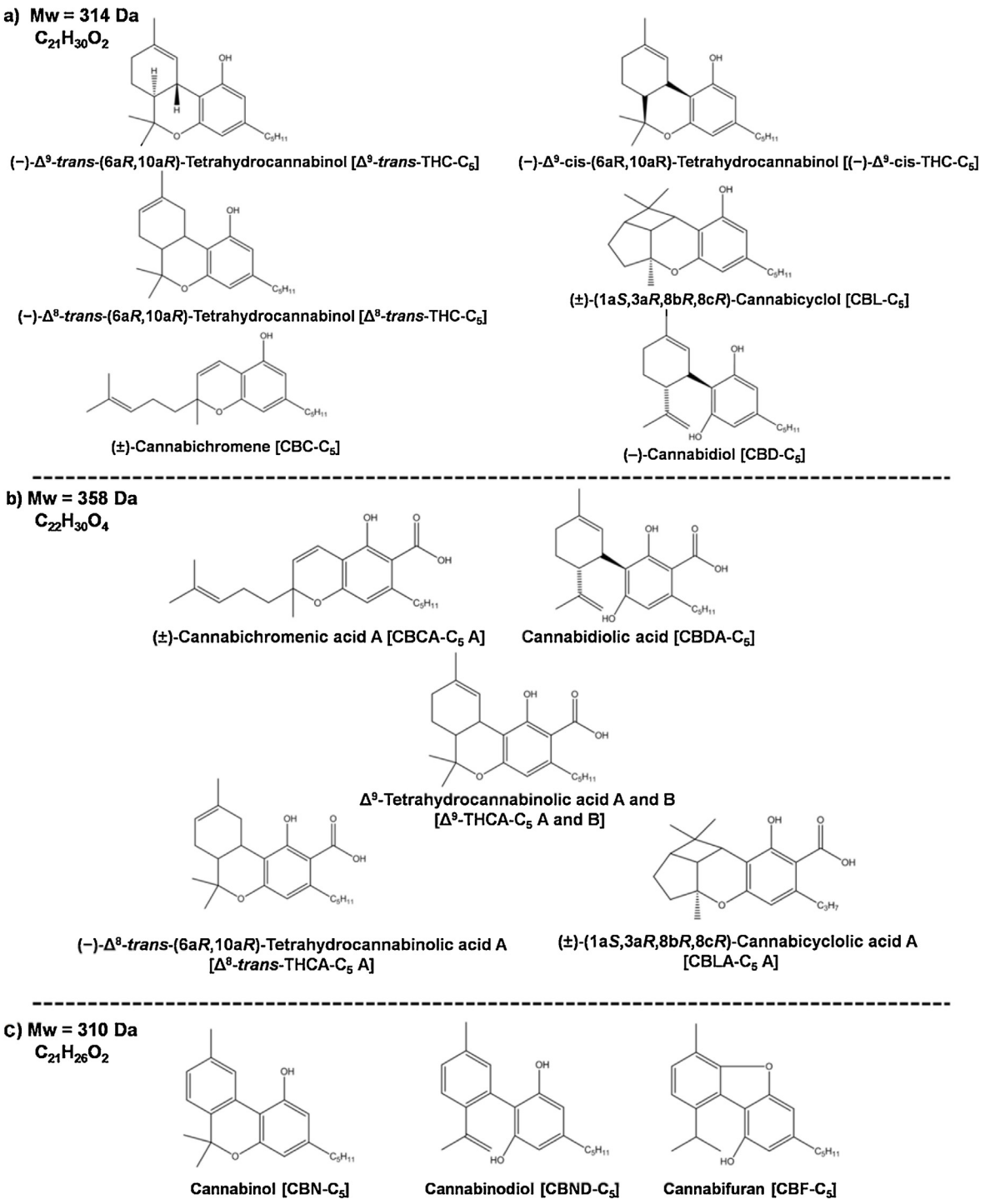

Fig. 1. Chemical structures of the main isomers of (a) Δ^9-*trans*-THC-C_5; (b) Δ^9-THCA-C_5; and (c) CBN-C_5.

decarboxylation during heating or smoking, resulting in its conversion to Δ^9-THC. In addition to Δ^9-THCA-A, four other isomers can exist, namely, CBDA-C_5 A, CBDA-C_5, Δ^8-*trans*-THCA-C_5 A, and CBLA-C_5 A, Fig. 1b [9–13].

Fig. 1c shows cannabidiol (CBN-C_5) and its isomers, the concentrations of which increase under storage or aging of marijuana owing to degradation of Δ^9–THC-C_5. Cannabinodiol (CBND) and cannabifuran (CBF-C_5), derived from CBD-C_5, are constitution isomers of CBN-C_5, with M_w = 310 Da [11–14].

The UNODC reports the marijuana is the most cultivated, trafficked, and consumed drug in the world. According to its 2015 annual report, around 182 million people consumed marijuana in 2013 [1]. In the same year, the amount of marijuana seized by authorities in Latin America and the Caribbean increased by 20–30%. However, overall, the amount of marijuana seized in North America was higher (47% of total) [15]. Thus, owing to matrix complexity, it is necessary to use new analytical methods with high sensibility and selectivity to identify the active ingredients presents in marijuana samples [16].

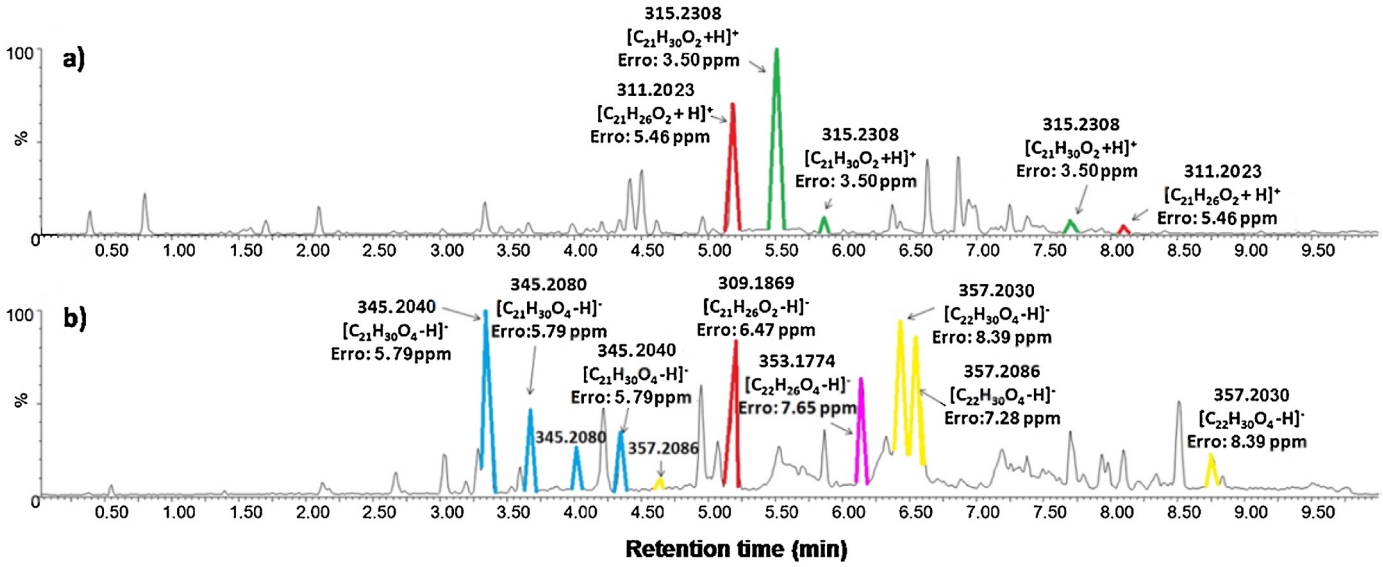

Fig. 2. Chromatograms for a typical hashish sample by (a) UPLC-ESI(+)-TWIM-MS, and (b) UPLC-ESI(−)-TWIM-MS.

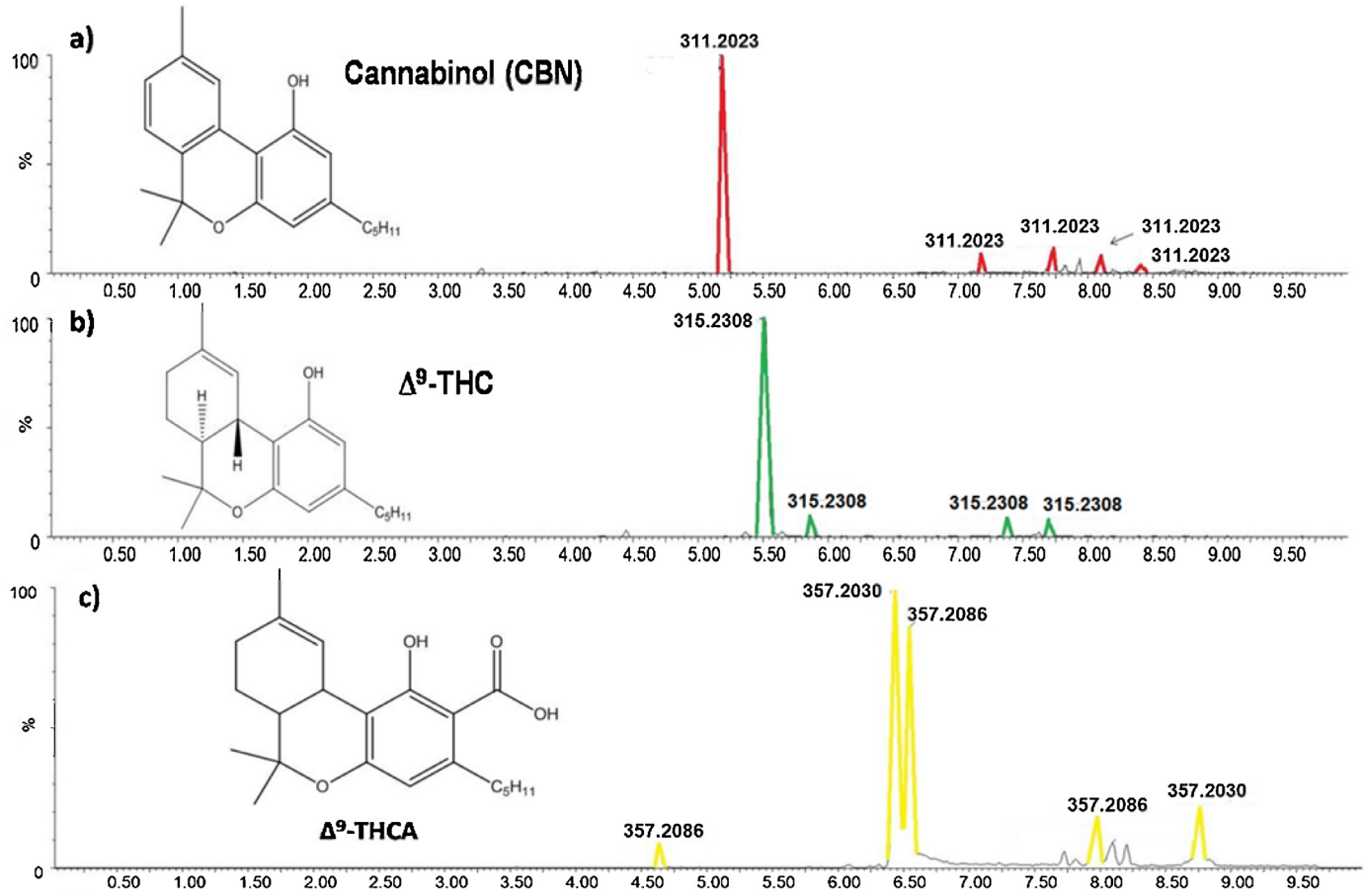

Fig. 3. Chromatograms of UPLC-ESI(±)-TWIM-MS in SIM mode for the ions at (a) *m*/*z* 311; (b) *m*/*z* 315 and (c) *m*/*z* 357.

In Brazilian forensic laboratories, cannabinoids are detected qualitatively by using the colorimetric test with fast blue BB salt. This test is based on the appearance of a specific color (usually pink) in the presence of Δ^9–THC-C_5, CBN-C_5, or CBD-C_5. According to Bordin et al., the colorimetric reactions occur owing to the phenolic nature of the chemical structure of cannabinoids [14]. Thus, this test is not specific because other phenolic compounds that might be present in the plants can lead to false-positive results [14,3]. In 2016, Romão et al. identified the products of the colorimetric reaction between fast blue BB salt and marijuana samples by using ultra-high resolution mass spectrometry (ESI(+)-Fourier transform ion cyclotron resonance mass spectrometry (FT-ICR MS)), thin layer chromatography (TLC), and UV–vis measurements. They also

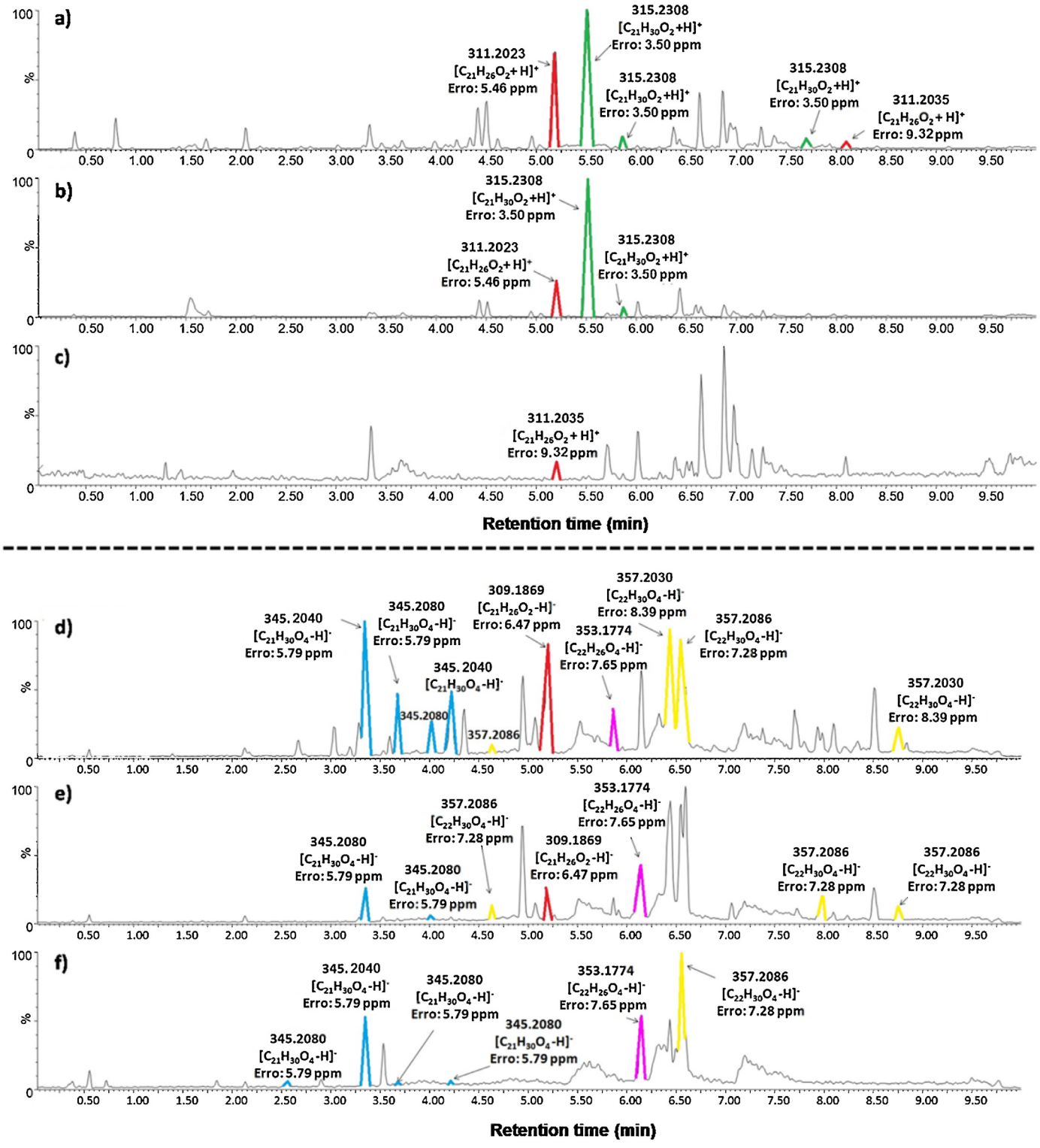

Fig. 4. Chromatograms of UPLC-ESI(+)-TWIM-MS and UPLC-ESI(−)-TWIM-MS for extracts of hashish ((a) and (d)), and of parts of the *Cannabis sativa* L. plant: flower ((b) and (e)), and leaf ((c) and (f)).

demonstrated that the fast blue BB salt has higher selectivity than other reagents such as fast blue B salt [6].

Among the popular techniques for analyzing cannabinoids, gas chromatography–mass spectrometry (GC–MS), which is used to characterize mainly Δ^9–THC-C_5 and its metabolites [17], stands out. GC–MS demonstrates excellent analytical performance, but this technique requires laborious sample preparation steps before instrumental analysis [17].

The use of more sophisticated techniques is also reported in literature, such as (FT-ICR MS) and matrix-assisted laser desorption/ionization imaging mass spectrometry (MALDI-IMS) [18]. Nascimento et al. found 21 cannabinoid species using ESI(−)-FT-

ICR MS. However, the main difficulty in cannabinoid identification by direct infusion, such as ESI(±), are your isomers [8].

Hyphenated analytical techniques such as liquid chromatography-electrospray ionization-tandem mass spectrometry (LC-ESI–MS/MS) allow differentiation and quantification of cannabinoid isomers with lower LOD and LOQ than those observed by GC-FID and GC–MS [19]. Schwope et al. performed MS/MS experiments on the main cannabinoid isomers (Δ^9–THC-C_5 and CBD-C_5), and both displayed the same fragmentation standard. However, these compounds were distinguished based on their retention times on the chromatographic column. In general, CBD elutes before Δ^9–THC [17]. In addition to the ESI source, other ionization sources at atmospheric pressure have been employed for studying cannabinoids owing to their lipophilic characteristics. Atmospheric pressure chemical ionization (APCI), for instance, presented lower LOD and LOQ values compared to the ESI source [20].

In addition to the above techniques, ion-mobility mass spectrometry (IM-MS) has been considered an innovative analytical tool for identifying isomeric compounds in complex matrices. This technique is based on the separation of ions based on the differences in their mobility in the gaseous phase in terms of charge, form, size, and molecular structure [21,22]. The separation occurs in a scale of milliseconds, which allows for coupling with the MS system, in which IMS can be easily coupled to TOF-MS analyzers [23]. IMS-MS can be coupled with traveling wave ion mobility mass spectrometry (TWIM-MS), being commercially available as Synapt G2-S HDMS. Another instrument is the Agilent 6560 Ion Mobility Q-TOF [24] that is conceptually simplest form of IMS based on a drift tume (DTIMS), where the ions are introduced (gated) into a cell consisting of a series of stacked electrodes filled with a static drift/buffer gas [25]. Both systems are also favorable from the viewpoint of coupling various chromatographic techniques and ionization sources before TWIM-MS analysis [26].

In 2013, Ahonen et al. used TWIM-MS as a fast and reproducible method for separating steroid isomers [25]. In 2015, Williams et al. investigated cancer metabolites in the intestinal epithelium by using TWIM-MS [27]. Fasciotti et al. compared the efficiencies of G1 (first generation) and G2 (second generation) Synapt TWIM-MS by varying the drift gas (N_2 and CO_2) [28]. The ionic mobilities of the sodiated forms $[M+Na]^+$ of four isomers of disaccharides (maltose, lactose, saccharose, and cellobiose) were evaluated. The separation was significantly better when using CO_2 as the drift gas than that when using N_2 [27].

Three studies have reported the use of TWIM-MS on samples of drugs prone to abuse. Romão et al. applied ESI(+)-TWIM-MS to distinguish three position isomers of chlorophenylpiperazine (*o*-CPP, *m*-CPP and *p*-CPP), sold frequently as ecstasy tablets. The ionic mobility of *o*-CPP allowed for its distinction from its isomers *m*-CPP and *p*-CPP by using CO_2 as the drift gas [29].Armenta et al. used TWIM-MS to detect and identify new psychoactive substances (phenethylamines, cathinones, synthetic cannabinoids, and tryptamines) [30]. Finally, Gwak and Almirall studied 35 new psychoactive substances by using Dt-IMS. However, there are no reports on the application of TWIM-MS for separating isomers of natural cannabinoids [24]. Thus, in this work, we aim to detect the presence of isomers of Δ^9-*trans*-THC-C_5, Δ^9-THCA-C_5, and CBN-C_5 in marijuana and hashish samples, and parts of the *Cannabis sativa* L. plant (flower and leaf) by employing UPLC-TWI-MS (Synapt G2-S HDMS) and direct infusion using TWIM-MS.

1.1. Methodology

1.1.1. Samples and reagents

Under a cooperation agreement with the Civil Police of Espírito Santo, Brazil, five samples of marijuana, parts of the *Cannabis sativa* L. plant (flowers and leaves), and hashish (concentrated extract of Δ^9–THC-C_5) were obtained. Acetonitrile (ACN), analytical grade purity >99.5% (*Vetec Química Fina*, Ltda, Brazil), was used for cannabinoid extraction and Synapt G2-S HDMS analysis. Sodium formate and Leu-enk, analytical grade purity >99.99% (Sigma-Aldrich Chemicals, USA), were used to calibrate Synapt G2-S HDMS.

Table 1
Parameters of the ESI source and of the ionic mobility cell.

Parameters	ESI(−)	ESI(+)
Capillary voltage	2.5 kV	3.5 kV
Source temperature	90 °C	90 °C
Cone voltage	40 V	50 V
Desolvation temperature	150 °C	200 °C
Desolvation gas flow rate (N_2).	500 L/h	500 L/h
Scanning rate	0.1 s/scan	0.1 s/scan
Traveling wave height	29.0 V	40.0 V
Traveling wave speed	650 m/s	652 m/s
Nitrogen pressure (driftgas)	2.90 mbar	2.90 mbar

1.2. Sample preparation

Around 2 mg of each sample was placed in different microtubes containing 1 mL of ACN, and then the solution was subjected to an ultrasonic bath for 15 min. After extraction, 100 μL of the solution was diluted in 900 μL of ACN to perform UPLC–MS and TWIM-MS analyzes using the ESI source on both positive and negative ionization modes, that is, ESI(+) and ESI(−), respectively. The mass spectrometer was a Synapt G2-S HDMS (Waters, Manchester, UK) with a chromatograph UPLC-I Class (Waters, Manchester, UK).

1.3. UPLC-ESI(±)-TWIM-MS and ESI(±)-TWIM-MS

The MS system comprised a UPLC-I Class (Waters Acquity – Waters, Milford, MA, USA) interconnected to the mass spectrometer by TWIM-MS, Synapt G2-S HDMS (high-definition mass spectrometer, Waters Corporation, Manchester, UK). This equipment had hybrid geometry, comprising quadrupole and time-of-flight (Q-TOF) analyzers. The chromatography was run in a binary solvent gradient, ratio A/B (phase A = water/formic acid 0.1% v/v; phase B = methanol/formic acid 0.1% v/v). The column used was a Acquity UPLC HSS T3 1.8 mm, 2.1 × 100 mm (Waters Corp., Milford, US) at 55 °C and with a flow rate of 0.500 mL min^{-1}. The gradient conditions were as follows: 10% phase B in 0 min; 60% phase B in 8 min; 95% phase B in 10 min; 95% phase B in 12 min; and after 2 min, the analysis returns to initial condition. The TOF analyzer operated with are resolving power $m/\Delta m_{50\%}$ = 45,000 (where $m/\Delta m_{50\%}$ is the full peak width that half-maximum peak height of $m/z \approx 400$),and it was calibrated in the m/z range of 100–700 by using a solution of sodium formate at 0.1% in acetonitrile/water 1:1 (v/v%). Leu-enk was used as the external standard solution. In the ion mobility cell, the original aperture of 2 mm was kept unchanged. The ion-transfer and ion-accumulation cells were operated at a pressure of 10^{-2} mbar of argon. N_2 gas was used in the mobility and ion separation experiments. Data acquisition and processing were performed in *Mass Lynx* 4.1 software (*Waters Corporation*). The parameters of the ESI source and the ion mobility cell are listed in Table 1.

The molecules presented in Table 1 were building using Avogadro [31], followed by classical energy minimization using steepest descent algorithm and UFF Force Field. These initial structures were optimized at the B3LYP/6-31G(d,p) theory level using the Gaussian 09 quantum chemistry package [32]. VMD program [33] was used to visualize the final results of geometry optimization calculations. Atomic partial charges were obtained with CGenFF

Table 2
m/z measured and theoretical values, molecular formula and retention time in the hashish sample by UPLC-ESI(±)-TWIM-MS.

measured *m/z*	Theoretical *m/z*	$[M+H]^+$ or $[M+H]^-$	Retention time (min)
311.2023	311.2006	$[C_{21}H_{26}O_2+H]^+$	5.18; and 8.12
315.2308	315.2319	$[C_{21}H_{30}O_2+H]^+$	5.48; 5,87; and 7.70
309.1869	309.1849	$[C_{21}H_{26}O_2-H]^-$	5.21
345.2040; 345.2080	345.2060	$[C_{21}H_{30}O_4-H]^-$	3.35; 3.65; 4.05; and 4.35
357.2030; 357.2086	357.2060	$[C_{22}H_{30}O_4-H]^-$	4.68; 6.43; 6.57; and 8.81

Table 3
Resolving power (Rp), separation factor (α) and peak-to-peak resolution (R_{p-p}) obtained from TWIM-MS data.

Ionization source	*m/z*	Drift time (ms)	Rp	Isomer pair	α	R_{p-p}
ESI(−)	357 (Δ^9-THCAA)	0.83 (A)	0.47	B; A	1.90	0.19
		1.58 (B)	0.44	B; C	1.47	
		2.33 (C)	0.89	C; A	2.81	
	313 (Δ^9-THC)	0.83 (A)	0.45	B; A	2.00	0.17
		1.66 (B)	0.43	B; C	1.45	
		2.41 (C)	0.69	C; A	2.90	
	311 (CBN)	3.69 (A)	0.72	B; A	1.26	0.10
ESI(+)		4.65 (B)	0.79	B; A	1.26	
	315 (Δ^9-THC)	2.47 (A)	0.63	B; A	1.76	0.10
		4.36 (B)	0.36	B; C	1.28	
		5.57 (C)	0.39	C; A	2.25	

program [34]. The MOBCAL program [35,36] was used to estimate the collision cross sections (Ω) of the optimized molecules at 300 K. We first applied three different methodologies: project approximation (PA), exact hard sphere scattering (EHSS) and trajectory method (TM) for He drift gas. However, we observed that these estimates do not well correlate with our experimental results. For example, CBN—C5 isomers (*m/z* 310) does not show significant Ω differences (Table 1S of the Supplementary material), as showed in the experimental mobility's profiles of Fig. 6. These discrepancies between experimental data and theoretical calculations are, most likely, due to fact that N_2 drift gas was used for TWIM-MS experiments while the initial calculations were performed using He gas. Thus, a modified version of MOBCAL [37] was used to estimates proper Ω values in nitrogen drift gas. This version takes into account ion-quadrupole interactions and the orientation of non-spherical gases during collisions. The number of trajectories for the TM-N_2 method was 250,000, which gave us accurate Ω values with a maximum standard deviation of 0.09 Å^2.

2. Results

2.1. UPLC-ESI(±)-TWIM-MS

Fig. 2a and b shows the chromatograms obtained from UPLC-TWIM-MS in the full-scan acquisition mode for the hashish extract analysis by using ESI(+) and ESI(−), respectively, which use the UPLC system coupled to ion mobility to separate the main cannabinoids and its isomers, simultaneously. Signals of *m/z* 315 and 311 for ESI(+) and 345, 309, 353 and 357 for ESI(−) were detected, and they correspond to the isomeric mixture of cannabinoids, as listed in Table 2. In the ESI(+) mode, three peaks were identified referring to the $[C_{21}H_{30}O_2+H]^+$ ion at *m/z* 315 with retention times of t = 5.48, 5.87, and 7.70 min, and two peaks corresponding to the $[C_{21}H_{26}O_2+H]^+$ ion at *m/z* 311 with t = 5.18 min and 8.12 min. The mass error varied from 3 to 6 ppm, as shown in Fig. 2a. The intense peaks at 5.48 min (*m/z* 315) and 5.18 min (*m/z* 311) probably indicate the presence of cannabinoids Δ^9-THC and CBN, respectively, because hashish is known to contain high concentrations of Δ^9-THC, and CBN, that is a by-product of Δ^9-THC degradation [38,39]. Besides, they have similar elution times (t = 5.48 and 5.18, respectively). Therefore, the remaining peaks correspond to their respective isomers (t = 8.12 min: CBND or CBF; and t = 5.87 and 7.70: (−)-*cis*- Δ^9-THC, Δ^8-*trans*-THC,CBL-C_5, CBC-C_5,CBD-C_5, or CBG-C_5).

Analyzing the chromatograms in the negative ionization mode, ESI(−), as in Fig. 2b, the CBN molecule is detected again, now in its deprotonated form, as the $[M-H]^-$ ion at *m/z* 309 and t = 5.18 min and as one of most abundant species. Three other ions having *m/z* 345, 353, and 357 were also found. Among them, only the $[C_{22}H_{26}O_4-H]^-$ ion at *m/z* 353.1774 and mass error = 7.7 ppm was identified as cannabinolic acid (CBNA). For the ions at *m/z* 345 (t = 3.35, 3.65, 4.05, and 4.35 min) and 357 (t = 4.68, 6.43, 6.57, and 8.81 min), various constitutional isomers or isobars can exist, with six chemical structures at most. The two ions detected at *m/z* 345.2080 are reported in the literature as isomers of cannabielsoic acid (CBEA-C_5 A or CBEA-C_5 B), while the $[C_{22}H_{30}O_4-H]^-$ ions at *m/z* 357.2086 can refer to CBDA, Δ^9-THCA-C_5 A/B, Δ^8-THCA-C_5A, CBLA-C_5 A, or cannabicromenic acid. The peak at t = 6.57 min probably corresponds to Δ^9-THCA-C_5 A/B, which is the precursor of Δ^9-THC. In general, the ions are detected with a mass error of 5–9 ppm.

To confirm the chemical connectivity of the peaks corresponding to the isomeric compounds of *m/z* 315 and 357, CID experiments were performed, and the results are shown in the Supplementary material (Figs. 1S–4S). All three isomers have similar fragmentation profiles, with a major fragment at *m/z* 193, followed by the ions at *m/z* 259 and 123 [3,8,40]. The signal at *m/z* 259 (*m/z* 315 → 259 transition) is explained by cleavage of the lateral chain (pentyl group) with a neutral loss of C_4H_8 (butene), 56 Da [8]. The intense signal at *m/z* 193 (*m/z* 315 → 193 transition) is explained by the neutral loss of C_9H_{14}, 122 Da. These results agree with those in the literature for the Δ^9-THC and CBD-C_5 structures [3,8]. Fig. 2S shows the proposed fragmentation mechanisms of the isomers Δ^9-THC, *trans*-CBG-C_5, and CBC-C_5. For Δ^9-THC and its optical isomers, the CID experiment, Fig. 1S(I), corroborated the proposed mechanism, Fig. 2S(I). In the second ESI(+)MS/MS spectrum, Fig. 1S(II), a typical transition leads to the formation of the fragment at *m/z* 175 owing to successive alkene losses via hydrogen rearrangement, and the fragment refers to the *trans*-CBG-C_5 compound, Fig. 2S(II). At last, the CID spectrum shown in Fig. 1S(III) confirms the presence of the compound CBC-C_5 based on to the presence of the ion at *m/z* 233, which was formed by the elimination of an alkene. In general, the presence of reference material is necessary for the unequivocal identification of Δ^9-THC and its isomers.

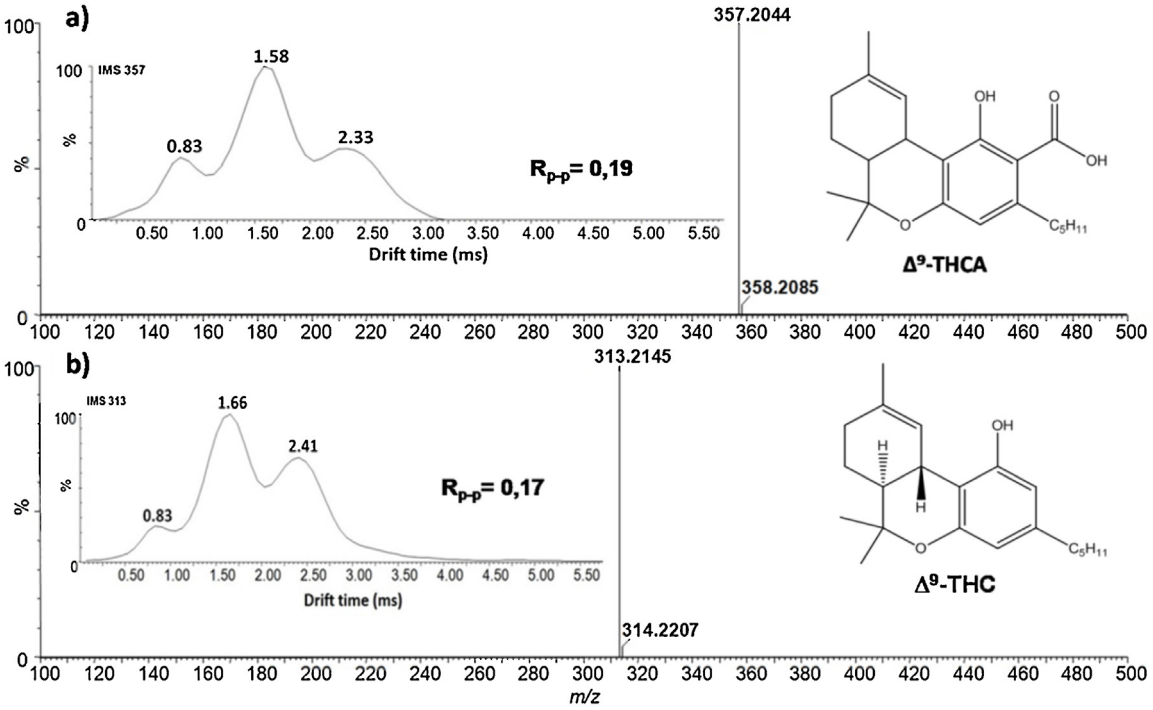

Fig. 5. Mobility profile for the ions at *m/z* (a) 357 and (b) 313 obtained by ESI(−)-TWIM-MS. In both cases is notable the isomeric separation of the three compounds.

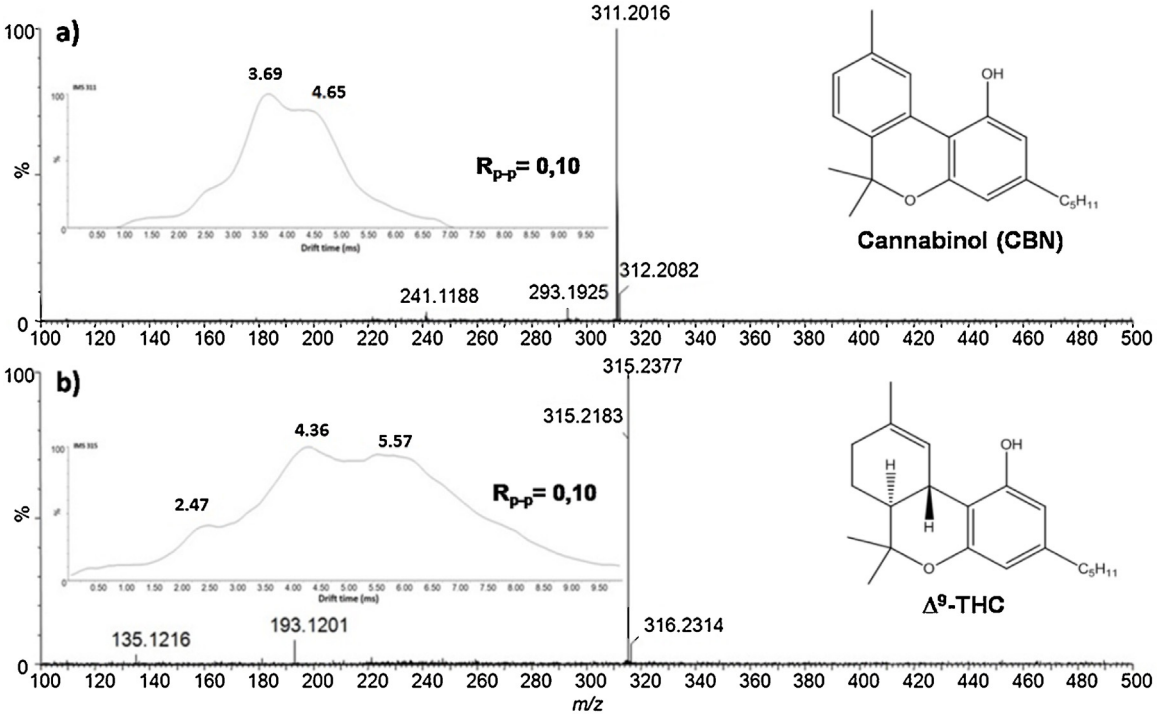

Fig. 6. Mobility profile for the ions at *m/z* (a) 311 and (b) 315 obtained by ESI(+)-TWIM-MS. Similar to Fig. 5, three isomers can be separated from ions of *m/z* 311 (6a) and *m/z* 315 (6b).

ESI(−)-MS/MS experiments for the ion at *m/z* 357 were performed as well, and the results are shown in Fig. 3S. A typical neutral loss of CO_2 (44 Da), leading to generation of the fragment at *m/z* 313 (Δ^9-THC and isomers), is detected in the most of the mass spectra shown in Fig. 3**S,** thus proving the presence of a carboxylic acid group in the structure of Δ^9-THC-A and its isomers. Moreover, the loss of H_2O (18 Da) generates the fragment at *m/z* 339 [8]. Other losses with more intense peaks were also observed, such as 32 Da (*m/z* 357 → 325 transition) and 183 Da (*m/z* 357 → 174 transition). These losses are mainly characteristic of the Δ^9-THCA, Δ^8-THCA, and CBDA structures [10,8]. Proposed mechanisms for the fragmentation of Δ^9-THCA and CBDA are shown in Fig. 4**S**. In this case,

Table 4
Theoretical collision cross section (Ω) using trajectory method (TM) and N_2 gas at 300 K.

M_w (Da)	Molecular Formula	Molecule	Ω_{TM} (N_2)/Å^2
314.	$C_{21}H_{30}O_2$	Δ^9-*trans*-THC-C_5	170.1
		Δ^9-*cis*-THC-C_5	170.8
		Δ^8-*trans*-THC-C_5	170.5
		CBL-C_5	167.9
		CBC-C_5	179.6
		CBD-C_5	173.8
358	$C_{22}H_{30}O_4$	CBCA-C_5 A	189.5
		CBDA-C_5	185.2
		Δ^9-THCA-C_5 A and B	179.6
		Δ^8-*trans*-THCA-C_5 A	180.5
		CBLA-C_5 A	177.4
310	$C_{21}H_{26}O_2$	CBN-C_5	171.8
		CBND-C_5	174.9
		CBF-C_5	168.9

the produced fragments from CID experiments, Fig. 3S, are similar, and no definitive conclusion connecting retention time and the chemical structures of these species can be drawn.

To improve selectivity and sensibility of UPLC-TWIM-MS for the detection of isomeric mixtures of cannabinoids, chromatograms were also acquired in the single-ion monitoring (SIM) mode for the ions at *m/z* 311, 315, and 357.

Fig. 3a–c shows the chromatograms in the SIM mode for the ions at *m/z* 311, 315, and 357, respectively, obtained using UPLC-ESI(±)-TWIM-MS. In Fig. 3a, five peaks are seen corresponding to the ion at *m/z* 311. In addition to the two isomers detected previously at t = 5.18 and 8.12 min, Fig. 2a, three additional peaks of lower intensities are seen at t = 7.19, 7.74 and 8.40 min. Therefore, a total of five isomers are identified, and this number is higher than the constitutional isomers reported in Fig. 1c. For the ion at *m/z* 315, an additional peak is identified at t = 7.38 min, resulting in the detection of three isomers of Δ^9-THC, Fig. 3b. Therefore, four of the six possible isomers (Δ^9-THC-C_5, CBD-C_5, CBL-C_5, Δ^9-*cis*-THC-C_5, Δ^8-*trans*-THC-C_5, and CBC-C_5) are identified, Fig. 1a. For the ion at *m/z* 357, whose precursor molecule is Δ^9-THC and retention time 6.57 min (Δ^9-THCA-C_5 A/B), other isomer/isobars with lower abundance are present at t = 7.95 min, resulting in a total of five compounds with *m/z* 357.

Fig. 4a–f shows the chromatograms of UPLC-ESI(+)-TWIM-MS (4a–c) and UPLC-ESI(−)-TWIM-MS (4d–f) for the hashish extracts (4a) and (4d), and parts of the *Cannabis sativa* L. plant (flower: (4b) and (4e); leaf: (4c) and (4f)). Note that a higher amount of cannabinoids is identified in the hashish, followed by flower and leaf. Using UPLC-ESI(+)-TWIM-MS, the ions at *m/z* 311 and 315 (t = 5.18 and 5.48 min, respectively) were detected as the majority compounds in the hashish extracts and the flower, while for the leaf extract, only the ion at *m/z* 311 was found. UPLC-ESI(−)-TWIM-MS results show that the ion at *m/z* 357 is the majority in all cases (t = 6.43 and 6.57 min).

Δ^9–THC can be found in different parts of the plant at various percentages: i) 20–60 wt% in hashish;[33] ii) 10–12 wt% in flowers; ii) 1–2 wt% in leaves; iii) 0.1–0.3 wt% in stalks; and iv) <0.03 wt% in roots [41,42]. These values agree with the observed high-intensity peaks corresponding to Δ^9-THC, its precursor (Δ^9-THCA-C_5, *m/z* 357), and by product of degradation (CBN, *m/z* 311 or 309) [8,43].

Five marijuana samples were also analyzed by UPLC-ESI(±)-TWIM-MS, Fig. 5S. In the ESI(+) mode, the $[C_{21}H_{26}O_2 + H]^+$ ion at *m/z* 311 is ever abundant and detected at t = 5.18 min, while in the ESI(−) mode, a higher amount of cannabinoid compounds is observed (signals at *m/z* 309, 345, 353 and 357). Similar to the ESI(+) results, the CBN ion is detected at *m/z* 309 (t = 5.21 min), Fig. 5S. Different from the results shown in Fig. 4, Δ^9-THC is detected in low concentration, Fig. 5S. This can possibly be ascribed to degradation of the compound, leading to its conversion to CBN molecules. Additionally, cannabinoid dimers (*m/z* 637 (328 + 310 Da), 653 (326 + 328 Da), and 681 (354 + 328 Da)) were also identified in the ESI(−) mode, such as the $[M+N-H]^-$ ion, where M and N correspond to different cannabinoids [8]. These results agree with the results of Nascimento et al., who affirmed that the presence of these species can be explained by the formation of covalent bonds via deprotonating of phenolic groups (Δ^9-THC, CBN, etc.) with carboxylic groups (Δ^9-THCA and its isomers) [8].

3. TWIM-MS

Among the samples explored, the hashish extract is notably rich in isomeric mixtures of cannabinoids, which makes it ideal for evaluating the performance of the TWIM-MS technique in the separation of said mixtures.

Initially, the separation of ions with the same *m/z* is possible only if there are differences in conformation, spatial configuration, or charge between species. The MS technique measures the *m/z* ratio of ions, while IMS attributes a drift time spectrum for each *m/z* value, creating a new dimension of data [44]. When determining the ionic mobility of an isomeric mixture, it is important to calculate the resolution (R_{p-p}) between the peaks of mobility. However, R_{p-p} depends on the separation factor between the peaks (α), defined as follows:

$$\alpha = \frac{td_2}{td_1} \quad (1)$$

An important feature of this work is comparison of the performance of TWIM-MS with that of UPLC-TWIM-MS considering that the former is faster in terms of analysis and does not require previous physical separation of the sample.

Figs.5a–b and 6 a–b show the drift times for the ions at *m/z* 357 (**5a**) and (**5b**) *m/z* 313 ($[M-H]^-$ species obtained using ESI(−)), and those for the ions at *m/z* 311 and 315 ($[M+H]^+$ species obtained using ESI(+)), respectively. Isomeric separation of the three compounds was observed in most of the cases. Table 3 lists the R_p for each peak, which varies from 0.36 to 0.89, as well as the values of α and R_{p-p}, where α > 1 indicates satisfactory separation between the peaks by ionic mobility.

The ions at *m/z* 357 and 313, Fig. 5a–b, show similar drift time profiles (detection of three ionic mobility peaks) with the most abundant drift time values at 1.58 and 1.66 ms, respectively. These values might correspond to the Δ^9-THCAA and Δ^9-THC species, respectively. Moreover, better isomeric separation efficiency is achieved in the ESI(−) mode, Fig. 5, compared to that in the ESI(+) mode, Fig. 6, as evidenced by the α values obtained from the ratios between isomer pairs, Table 3.

The ESI(+)TWIM-MS results for the ions at *m/z* 311 and 315, Fig. 6, show lower chromatographic resolutions (compare R_{p-p} and

α values in Table 3). The drift time profiles of Δ^9-THC and its isomers were similar in both ionization modes, Figs. 5b and 6b.

The results of the calculations of CCS (Å2) to isomers of the ions of *m/z* 310, 314 and 358 are shown in Table 4, having N_2 as drift gas. Comparing the CCS values among the isomers of Δ^9-THC (314 Da), they can be ordered as follows: CBL-C_5 < Δ^9-*trans*-THC-C_5 ~ trans-Δ^8-THC-C_5 ~ *cis*-Δ^9-THC-C_5 < CBD-C_5 < CBC-C_5. Associating to results of Table 4 with those of Figs.5b and 6b, note that the peak of higher abundance presents intermediate value of drift-time (1.66 and 4.36 ms, Figs.5b and 6b, respectively) can correspond to Δ^9-*trans*-THC-C_5. Similar result was obtained for the precursor of Δ^9-*trans*-THC, the Δ^9-THCA-C_5 (358 Da), where the isomers of ion of *m/z* 358 obey the following order of CCS values: CBLA-C_5 A < Δ^9-THCA-C_5 A and B ~ Δ^8-transTHCA-C_5 A < CBDA-C_5 < CBCA-C_5 A. This result suggests that the Δ^9-THCA-C_5 and B has a drift-time of 1.58 ms, Fig. 5a. Finally, the isomers of ion of *m/z* 311 show the following order of CCS values: CBF-C5 < CBN-C5 < CBND-C5, corresponding to drift-times of 2.52, 369, and 4.65 ms, respectively, Fig. 6a.

4. Conclusion

Ultra performance liquid chromatography (UPLC) coupled to mass spectrometry as well as traveling wave ion mobility mass spectrometry (TWIM-MS) were applied to hashish samples, marijuana, and parts of the *Cannabis sativa* L. plant (flower and leaf) to identify the presence of a complex isomeric mixture containing mainly cannabinoids such as Δ^9-THC, cannabidiol (CBNC_5, M_w = 310 Da), and Δ^9-tetrahydrocannabinolic acid A and B (Δ^9-THCA-C_5 A/B, M_w = 358 Da). A maximum of three isomers were identified for the ions at *m/z* 315/313, 311, and 357 by using the ESI-TWIM-MS technique, while higher selectivity was observed when using UPLC-ESI-TWIM-MS, in which isomeric separation between four to five compounds was achieved in the SIM ion-acquisition mode. The main ions found corresponded to CBN-C_5, Δ^9-THC, cannabielsioc acid, Δ^9-THCA-C_5, and their isomers. To confirm the structure of the cannabinoids, MS/MS experiments were performed, and we proposed a fragmentation mechanism for the ions at *m/z* 315 and 357. However, the similarity between fragmentation profiles hampered discrimination of the isomers at *m/z* 357. Future studies (part II of this manuscript) will be developed by using reference standards of cannabinoids to identify and quantify their isomeric species.

Acknowledgments

The authors thank FAPES (65921380/2013), CAPES (23038.007083/2014-40), and CNPq (445987/2014-6) for financial support.

Appendix A. Supplementary data

Supplementary data associated with this article can be found, in the online version, at http://dx.doi.org/10.1016/j.ijms.2016.10.018.

References

[1] United Nations Office on Drugs and Crime –UNODC, Vienna World Drug Report. Retrieved 20 2015 from http://www.unodc.org/wdr2014/ (2014).
[2] M.R. Boleda, M.T. Galceran, F. Ventura, Trace determination of cannabinoids and opiates in waste water and surface waters by ultra-performance liquid chromatography–tandem mass spectrometry, J. Chromatogr. A 1175 (2007) 38–48.
[3] M.A. Elsohly, D. Slade, Chemical constituents of marijuana: the complex mixture of natural cannabinoids, Life Sci. 78 (2005) 539–548.
[4] F. Zulfiqar, S.A. Ross, D. Slade, S.A. Ahmed, M.M. Radwan, Z. Ali, I.A. Khan, M.A. Elsohly, Cannabisol, a novel Δ-9-THC dimer possessing a unique methylene bridge, isolated from Cannabis sativa, Tetrahedron Lett. 53 (2012) 3560–3562.
[5] T. Yamauchi, Y. Shoyama, H. Aramaki, T. Azuma, I. Nishioka, Tetrahydrocannabinolic acid, a genuine substance of tetrahydrocannabinol, Chem. Pharm. Bull. 15 (1967) 1075.
[6] N.A. Santos, L.M. Souza, E. Domingos, H.S. França, V. Lacerda Jr., A. Beatriz, B.G. Vaz, R.R.T. Rodrigues, V.V. Carvalho, B.B. Merlo, R.M. Kuster, W. Romão, Evaluating the selectivity of colorimetric test (Fast blue BB salt) for the cannabinoids identification in marijuana street samples by UV-Vis, TLC ESI(+)MS and ESI(+)MS/MS, Foren. Chem. 1 (2016) 13–21.
[7] A.W. Zuardi, J.A.S. Crippa, J.E.C. Hallak, F.A. Moreira, F.S. Guimarães, Cannabidiol, a Cannabis sativa constituent, as an antipsychotic drug, Braz. J. Med. Biol. Res. 39 (2006) 421.
[8] I.R. Nascimento, H.B. Costa, I.M. Souza, L.C. Soprani, B.B. Merlo, W. Romão, Chemical identification of cannabinoids in street marijuana samples using electrospray ionization FT-ICR mass spectrometry, Anal. Methods 7 (2015) 1415–1424.
[9] F.E. Dussy, C. Hamberg, M. Luginbul, T. Schwerzmann, T. Briellman, Isolation of Delta9-THCA-A from hemp and analytical aspects concerning the determination of Δ^9-THC in cannabis products, Forensic Sci. Int. 3 (2005) 149.
[10] L. Bijlsma, J.V. Sancho, F. Hernández, W. Niessen, Fragmentation pathways of drugs of abuse and their metabolites based on QTOF MS/MS and MSE accurate-mass spectra, J. Mass Spectrom. 46 (2011) 865–875.
[11] M.M. Halldin, S. Carlsson, S.L. Kanter, M. Widman, S. Agurell, Urinary metabolites of delta 1-tetrahydrocannabinol in man, Arzneimittelforschung 32 (1981) 764–768.
[12] R. Andrews, S. Paterson, A validated method for the analysis of cannabinoids in post-mortem blood using liquid–liquid extraction and two-dimensional gas chromatography?mass spectrometry, Foren. Sci. Int. 222 (2012) 111–117.
[13] J. Jung, M.R. Meyer, H.H. Maurer, C. Neusuß, W. Weinmann, V. Auwarter, Studies on the metabolism of the Δ^9-tetrahydrocannabinol precursor Δ^9-tetrahydrocannabinolic acid A (Δ^9-THCA-A) in rat using LC-MS/MS, LC-QTOF MS and GC-MS techniques, J. Mass Spectrum. 44 (2009) 1423–1433.
[14] D.C. Bordin, M. Messias, R. Lanaro, S.O.S. Cazenave, J.L. Costa, Análise forense: pesquisa de drogas vegetais interferentes de testes colorimétricos para identificação dos canabinóides da maconha (*Cannabis Sativa* L.), Quím. Nova 35 (2012) 2040–2043.
[15] United Nations Office on Drugs and Crime – UNODC, Recommended methods for the identification and analysis of cannabis and cannabis products. New York. Retrieved Jan. 2016, from http://www.unodc.org/documents/scientific/ST-NAR-40-Ebook.pdf (2009).
[16] J.T. Mosquera, Marihuana – cannabis – aspectos toxicologicos, clinicos, sociales y potenciales usos terapeuticos, UNODC (2015).
[17] D.M. Schwope, K.B. Scheidweiler, M.A. Huestis, Direct quantification of cannabinoids and cannabinoid glucuronides in whole blood by liquid chromatography–tandem mass spectrometry, Anal. Bioanal. Chem. 401 (2011) 1273–1283.
[18] K. Kuwayama, T. Yamamuro, K. Tsujikawa, H. Miyaguchi, T. Kanamori, Y.T. Iwata, H. Inoue, Utilization of matrix-assisted laser desorption/ionization imaging mass spectrometry to search for cannabis in herb mixtures, Anal. Bioanal. Chem. 406 (2014) 4789–4794.
[19] C. Lacroix, E. Saussereau, Fast liquid chromatography/tandem mass spectrometry determination of cannabinoids in micro volume blood samples after dabsylderivatization, J. Chromatogr. B 905 (2012) 85–95.
[20] S.B. Grauwiler, A. Scholer, J. Drewe, Development of a LC/MS/MS method for the analysis of cannabinoids in human EDTA-plasma and urine after small doses of Cannabis sativa extracts, J. Chromatogr. B 850 (2007) 515–522.
[21] G. Astarita, G. Paglia, K. Yu, Ion-Mobility Mass Spectrometry in Metabolomics and Lipidomics MS – The Practical Art. LC.GC Europe., Waters Corporation, USA, 2015 (September).
[22] A.B. Kanu, P. Dwivedi, M. Tam, I. Matz, H.H. Hill, Ionmobility-massspectrometry, J. Mass Spectrom. 43 (2008) 1–22.
[23] A.A. Shvartsburg, R.D. Smith, Fundamentals of traveling wave ion mobility spectrometry, Anal. Chem. 80 (2008) 9689–9699.
[24] S. Gwak, J.R. Almirall, Rapid screening of 35 new psychoactive substances by ion mobility spectrometry (IMS) and direct analysis in real time (DART) coupled to quadrupole time-of-flight mass spectrometry (QTOF-MS), Drug Test Anal. 7 (2015) 884–893.
[25] C.J. Gray, B. Thomas, R. Upton, L.G. Migas, C.E. Eyers, P.E. Barran, S.L. Flitsch, Applications of ion mobility mass spectrometry for high throughput, high resolution glycan analysis, Biochim. Biophys. Acta 1860 (2016) 1688–1709.
[26] L. Ahonen, M. Fasciotti, G.B. Gennäs, T. Kotiaho, R.J. Daroda, M.N. Eberlin, R. Kostiainen, Separation of steroid isomers by ion mobility mass spectrometry, J. Chromatogr. A 1310 (2013) 133–137.
[27] M.D. Williams, X. Zhang, A.S. Belton, L. Xian, T. Huso, J.J. Park, W.F. Siems, D.R. Gang, I.M.S. Resar, R. Reeves, H. Hill Jr., HMGA1 drives metabolic reprogramming of intestinal epithelium during hyperproliferation polyposis, and colorectal carcinogenesis, J. Proteome Res. 14 (2015) 1420–1431.
[28] M. Fasciotti, G.B. Sanvido, V.G. Santos, P.M. Lalli, M. McCullagh, G.F. de Sá, R.J. Daroda, M.G. Peter, M.N. Eberlin, Separation of isomeric disaccharides by traveling wave ion mobility mass spectrometry using CO2 as drift gas, J. Mass Spectrom. 47 (2012) 1643–1647.
[29] W. Romão, P.M. Lalli, M.F. Franco, G. Sanvido, N.V. Schwab, R. Lanaro, J.L. Costa, B.D. Sabino, M.I.M.S. Bueno, G.F. Sá, R.J. Daroda, V. Souza, M.N. Eberlin, Chemical profile of meta-chlorophenylpiperazine (m-CPP) in ecstasy tablets by easy ambient sonic-spray ionization X-ray fluorescence, ion mobility mass spectrometry and NMR, Anal. Bioanal. Chem. 400 (2011) 3053–3064.

[30] S. Armenta, S. Garrigues, M. La Guardia, J. Brassier, M. Alcalá, M. Blanco, C. Perez-Alfonso, N. Galipienso, Detection and characterization of emerging psychoactive substances by ion mobility spectrometry, Drug Test.Anal. 7 (2015) 280–289.
[31] M.D. Hanwell, D.E. Curtis, D.C. Lonie, T. Vandermeersch, E. Zurek, G.R. Hutchison, Avogadro: an advanced semantic chemical, editor, visualization, and analysis platform, J. Cheminform. 4 (1) (2012) 17.
[32] M. J. Frisch, G. W. Trucks, H. B. Schlegel, G. E. Scuseria, M. A. Robb, J. R. Cheeseman, G., Scalmani, V., Barone, B., Mennucci, G. A. Petersson, H., Nakatsuji, M., Caricato, X., Li, H. P. Hratchian, A. F. Izmaylov, J., Bloino, G., Zheng, J. L. Sonnenberg, M., Hada, M., Ehara, K., Toyota, R., Fukuda, J., Hasegawa, M., Ishida, T., Nakajima, Y., Honda, O., Kitao, H., Nakai, T., Vreven, J. A. Montgomery Jr., J. E. Peralta, F., Ogliaro, M., Bearpark, J. J. Heyd, E., Brothers, K. N. Kudin, V. N. Staroverov, R., Kobayashi, J., Normand, K., Raghavachari, A., Rendell, J. C. Burant, S. S. Iyengar, J., Tomasi, M., Cossi, N., Rega, J. M. Millam, M., Klene, J. E. Knox, J. B. Cross, V., Bakken, C., Adamo, J., Jaramillo, R., Gomperts, R. E. Stratmann, O., Yazyev, A. J. Austin, R., Cammi, C., Pomelli, J. W. Ochterski, R. L. Martin, K., Morokuma, V. G. Zakrzewski, G. A. Voth, P., Salvador, J. J. Dannenberg, S., Dapprich, A. D. Daniels, Ö., Farkas, J. B. Foresman, J. V. Ortiz, J., Cioslowski, D. J. Fox, *Gaussian 09, Revision E. 01; Gaussian*, (2009).
[33] W. Humphrey, A. Dalke, K.J. Schulten, VMD: visual molecular dynamics, Molec. Graph 14 (1996) 33.
[34] K. Vanommeslaeghe, A.D. MacKerell, Automation of the CHARMM general force field (CGenFF) I: bond perception and atom typing, J. Chem. Inf. Model 52 (2012) 3144.
[35] M.F. Mesleh, J.M. Hunter, A.A. Shvartsburg, G.C. Schatz, M.F. Jarrold, J. Phys. Chem 100 (40) (1996) 16082.
[36] A.A. Shvartsburg, M.F. Jarrold, Chem. Phys. Lett. 261 (1–2) (1996) 86.
[37] I. Campuzano, M.F. Bush, C.V. Robinson, C. Beaumont, K. Richardson, H. Kim, H.I. Kim, Anal. Chem. 84 (2) (2012) 1026.
[38] G.S. Lewis, C.E. Turner, Constituents of Cannabis sativa L. XIII: Stability of dosage form prepared by impregnating synthetic (−)-delta 9-trans-tetrahydrocannabinol on placebo Cannabis plant material, J. Pharm. Sci. 67 (1978) 876.
[39] M.A. Elsohly, Marijuana and the cannabinoids, in: Forensic Science and Medicine, Humana Press, 2007.
[40] M.M. Eiras, D.N. Oliveira, M.S. Ferreira, M. Benassi, S.O.S. Cazenave, R.R. Catharino, Fast fingerprinting of cannabinoid markers by laser desorption ionization using silica plate extraction, Anal. Methods 6 (2014) 1350–1352.
[41] Relatório anual Departamento de Polícia Federal. Relatório de atividades. Retrieved 01 Mar. 2015, from http://www.dpf.gov.br/institucional/relatorio-anual-pf/ (2008).
[42] M.E. Wall, B.M. Sadler, D. Brine, H. Taylor, M. Perez-Reyes, Metabolism, disposition, and kinetics of Δ^9-tetrahydrocannabinol in men and women, Clin. Pharmacol. Ther. 34 (1983) 352–363.
[43] K. Watanabe, S. Yamaori, T. Funahashi, T. Kimura, I. Yamamoto, Cytochrome P450 enzymes involved in the metabolism of tetrahydrocannabinols and cannabinol by human hepatic microsomes, Life Sci. 80 (2007) 1415–1419.
[44] M. Fasciotti, P.M. Lalli, G. Heerdt, R.A. Steffen, Y.E. Corilo, G.F. Sá, R.J. Dadora, F.A.M. Reis, N.H. Morgon, R.C.L. Pereira, M.N. Eberlin, C.F. Klitzke, Structure-drift time relationships in ion mobility mass spectrometry, Int. J. Ion Mobility Spectrom. 16 (2013) 117–132.